

Supporting Information

Jones et al. 10.1073/pnas.1405162112

SI Materials and Methods

Surgical Procedures. Surgery was performed using aseptic techniques under full general anesthesia for the implantation of the head post and recording chamber. Anesthesia was induced with aketamine/medetomidine mixture (6.4 mg/kg ketamine and 0.08 mg/kg medetomidine, i.m.), and i.v. access established after atropine administration (atropine sulfate 0.04 mg/kg i.m.). After intubation, anesthesia was maintained using isoflurane [1–2.5% (vol/vol)] in O₂. Blood pressure, electrocardiogram, end-tidal CO₂, rectal temperature, and peripheral oxygenation were continually monitored. A thermostatically controlled heat blanket was used to maintain body temperature at 37°C, and i.v. fluids were given as required. Animals were given s.c. injections of antibiotic (BetamoxLA, 0.1 mL/kg) and a nonsteroidal antiinflammatory (Meloxicam 0.2 mg/kg) at the commencement of the surgical procedure and also received oral antibiotic (Synulox palatable drops, 12.5 mg/kg, twice daily) and nonsteroidal antiinflammatory medication (meloxicam 0.1 mg/kg daily) for a minimum period of 5 d pre- and postsurgery. At the end of the surgical procedure, buprenorphine (0.01 mg kg⁻¹, i.m.) was administered for analgesia and repeated twice per day for up to 3 d as needed. Animals were recovered under supervision in protected and warm environments. The implantation of head post and chamber and the craniotomy were all performed in the same surgical procedure.

We used acrylic-free titanium implants (1) localized stereo-tactically after a full structural MRI scan to target the lateral geniculate nucleus. Chambers were custom-angled based on the MRI data to optimize placement on the skull.

Visual Stimulation. Visual stimuli were generated in Matlab (Mathworks Inc.), using the Psychophysics toolbox (2, 3) running a custom stimulus-generator (dx.doi.org/10.5281/zenodo.11080). This enabled high-quality random dot generation; all dots were spatially and positionally antialiased. Floating-point pixel values were used to specify position. This meant subpixel blending minimized artifacts where movement on screen is forced to the nearest integer pixel. Individual “pixels” thus have a more linear response (rounding does not cause them to suddenly light up). The gamma-corrected visual display was an Iiyama HM204DTCRT driven at a resolution of 1280×1024 pixels (with each pixel subtending a visual angle of 0.03°) at an 85-Hz vertical refresh rate; we used a DataPixx (VPixx Technologies Inc.) to extend contrast range up to 14 bits when necessary.

Electrophysiological recording. We recorded extracellular activity from LGN neurons using tetrodes (Thomas Recording; impedance range 0.5–0.9 MΩ) driven transdurally by a Thomas minimatrix system micromanipulator (Thomas Recording). The full wideband signal was amplified, high-pass filtered at 0.5 Hz, and stored along with temporally precise strobed words (display-locked with microsecond precision by the DataPixx, indicating stimulus and behavioral conditions) at 40 KHz, using an Omniplex recording system (Plexon Inc). Spike wave forms were then further band-pass-filtered from 250 to 8,000 Hz and thresholded using OfflineSorter software (Plexon Inc). We identified distinct single-unit and multiunit waveform clusters, using manually refined principal component analysis tetrodesorting methods in OfflineSorter. The resultant spike times along with the stimulus and behavioral markers were then analyzed using customized Matlab routines.

Microsaccade detection. To detect microsaccades, we used the velocity-based algorithm code from Engbert and Mergenthaler (4) that defines microsaccades as parts of the eye movement trajectory, where velocity exceeds a relative velocity threshold multiple (λ) of the median SD. We used a relative velocity threshold set to five median-based SDs of the velocity values observed ($\lambda=5$), a temporal threshold of two samples (8 ms), and a maximum angular excursion of $<1^\circ$.

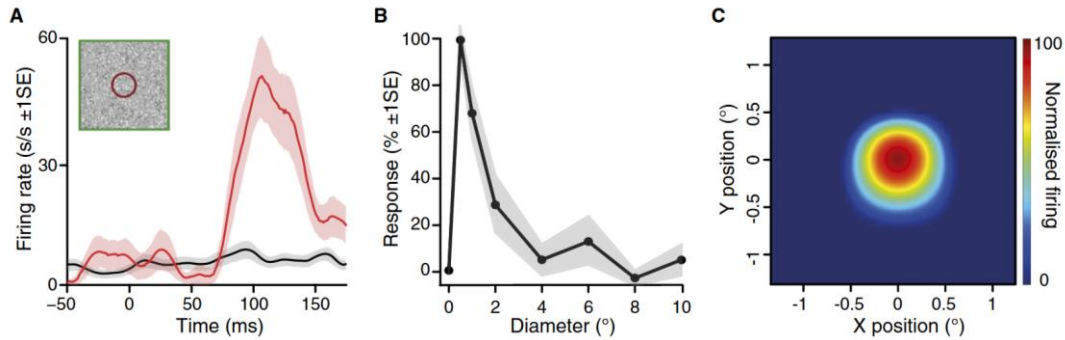


Fig. S1. Example figure-ground response together with the location and spatial extent of the cell's RF center. (A) Typical example of enhancement of neuronal firing when the figure, as opposed to the ground component of the stimulus, was located over the RF. SDF to figure (red) and ground (black) stimulus conditions overlying the RF. Time epoch commences 50 ms before stimulus motion onset and ends before saccade initiation. Shading indicates \pm 1 SE. Inset schematic denotes the size of the RF relative to the size of figure. Figure size 4° . (B and C) Area summation tuning curve (B) and surface map (C) documenting the location and extent of the cell's RF. The tuning curve in B plots the variation in response magnitude for increasing diameters of a flashed spot of light located over the RF, whereas the surface map in C plots the response to a 0.75° flashing spot presented at a range of locations in visual space encompassing the cell's RF locations. For both plots, responses were normalized with respect to the optimal evoked response. Shading in B indicates \pm 1SE.

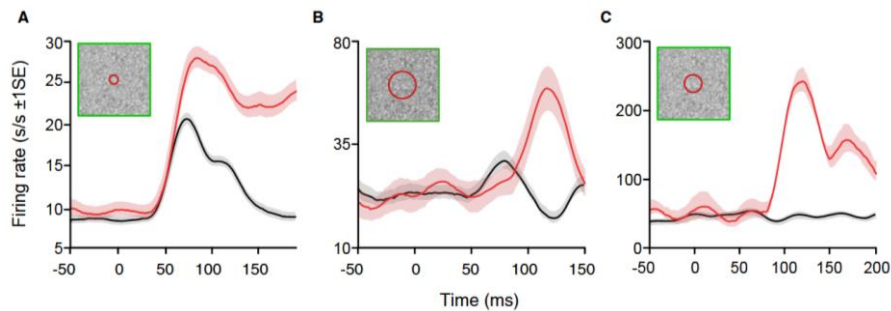


Fig. S2. Enhancement of neuronal firing when the figure, as opposed to the ground component of the stimulus, was located over the RF. (A) Response of an example LGN neuron showing an initial early transient response to the stimuli. SDF to figure (red) and ground (black) stimulus conditions (\pm 1 SE) overlying the RF. Time epoch commences 50 ms before stimulus motion onset and ends before saccade initiation. Inset schematic denotes the size of the RF relative to the size of figure. (B) Enhancement of neuronal firing to a figure located over the RF, when the figure was not the target for a saccade. Essentially, we added a second, identical target figure to our standard figure-ground task and rewarded the monkey for making a saccade to the location of either figure. The monkey could thus choose to saccade to either target, and this allowed us to record data when the figure located over the RF was not the target for a saccade. Color conventions as in A. (C) The monkeys fixated much more precisely on the fixation spot than demanded by the experimental fixation window, and robust FGM responses were maintained when we confined the data analysis to those trials where the monkeys maintained fixation within a small region of the fixation window. Example shows the response pattern for trials where fixation was confined within a 0.25° radius fixation window. Other conventions as in A.

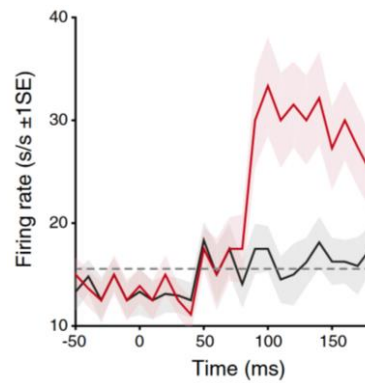


Fig. S3. Averaged population responses to figure (red) and ground (black) stimulus conditions overlying the RF, for our single unit cell sample ($n = 77$). Shading represents ± 1 SE. Motion onset occurred at time 0 ms. Horizontal dotted line denotes background plus 99% confidence limit. In contrast to the average population histograms shown in Figs. 2, 3, and 4, no normalization was applied to the individual data records before averaging.

1. Adams DL, Economides JR, Jocson CM, Parker JM, Horton JC (2011) A watertight acrylic-free titanium recording chamber for electrophysiology in behaving monkeys. *J Neurophysiol* 106(3):1581–1590.
2. Brainard DH (1997) The Psychophysics Toolbox. *Spat Vis* 10(4):433–436.3.
3. Pelli DG (1997) The Video Toolbox software for visual psychophysics: Transforming numbers into movies. *Spat Vis* 10(4):437–442.4.
4. Engbert R, Mergenthaler K (2006) Microsaccades are triggered by low retinal images lip. *Proc Natl Acad Sci USA* 103(18):7192–7197.